Regge Secondary Trajectories

G. C. Fox* AND L. Sertorio
Institute for Advanced Study, Princeton, New Jersey 08540
(Received 8 July 1968)

A systematic study of isospin-one exchange reactions leads to the proposal of additional singularities in the j plane of this channel. Such an analysis gives rise to several extra predictions to be tested in future experiments.

1. INTRODUCTION

IN the general development of the Regge-pole hypothesis the study of two-body reactions is at the most advanced level. Although this is not due to a fundamental reason, it happens in practice. A sufficient reason for this fact is that the simplest experimental measurements, two-body differential cross sections, bear a simple and very direct relation with the outcome of the Regge-pole hypothesis applied to two-body reactions. And phenomenology has been found to be vital for the development of the hypothesis. It follows that in the study of two-body reactions, we have a rather detailed understanding.

We catalog here the concepts which have very general validity and discuss their consequences.

(1) Method of Reggeization[1–4] or kinematics. The examination of what is meant by Reggeizing a two-body reaction for any mass and spin has led to a detailed Regge kinematics, viz.,

(a) the structure of the residues which is of double nature—evasive and conspiring;
(b) link among trajectories and residues at $t=0$ in the case of conspiracy;
(c) structure of the residues due to the α-factors (see Appendix A for terminology).

From the kinematics we derive the following: We must consider sets of reactions involving Regge-pole contributions with such quantum numbers that they are connected by points (a) and (b). Then factorization and (c) creates the most restrictive kinematical conditions. Such a set is the most economical, in the spirit of Regge theory. One example is the following, on which we will concentrate in this paper:

$$\begin{aligned} &(1)\ \pi^-p\to\pi^0n, && (5)\ \pi N\to A_1N,\\ &(2)\ \pi N\to\pi\Delta, && (6)\ \pi N\to A_1\Delta,\\ &(3)\ \pi N\to\omega N, && (7)\ \pi N\to A_2N,\\ &(4)\ \pi N\to\omega\Delta, && (8)\ \pi N\to A_2\Delta. \end{aligned} \tag{1}$$

Another set which involves just π and A_2 exchange is

$$\begin{aligned} &\pi N\to\eta N, && \pi N\to\rho\Delta,\\ &\pi N\to\eta\Delta, && \pi N\to f^0N,\\ &\pi N\to\rho N, && \pi N\to f^0\Delta, \end{aligned} \tag{1'}$$

while all $T=1$ poles (ρ,B,π,A_2,A_1) can be exchanged in

$$\begin{aligned} &K^-p\to\bar{K}^0n, && pn\to np, && \gamma N\to\pi N,\\ &KN\to K\Delta, && p\bar{p}\to n\bar{n}, && \gamma N\to\pi\Delta,\\ &KN\to K^*_{890,1400}N, && NN\to N\Delta, &&\\ &KN\to K^*_{890,1400}\Delta, && NN\to\Delta\Delta. && \end{aligned} \tag{1''}$$

As mentioned, a point of considering joint reactions is that one may attempt to test the important prediction of the factorization of Regge residues. Thus there is much interest in whether in addition to the well-known leading poles one needs cuts to explain the present data. It is difficult to test the different energy dependencies expected for cuts and poles since only in the reactions involving stable particles (e.g., πN charge exchange) is the normalization of the data known to sufficient accuracy. However, through the t behavior of $d\sigma/dt$ and, in particular, the density matrix elements of the decaying particle, the large number of resonance production experiments give important clues as to the nature of the underlying dynamics.

(2) Exchange degeneracy.[5,6] The possible consequences of the exchange degeneracy reflect a dynamical property. If exchange degeneracy is valid, extra connections are introduced among sets which, by kinematics only, are uncorrelated.

(3) Sum rules are also dynamical equations. They select particular helicity states and have obviously in principle more predictive power than points (1) and (2). We will use points (2) and (3) as restrictions or consistency requirements in discussing the set of reactions (1).

A rather well-established feature which emerges from the analysis of reactions (1) is the existence of the ρ trajectory and, with less detail, the B trajectory.[7]

* Research supported by the National Science Foundation.

[1] G. Cosenza, A. Sciarrino, M. Toller, University of Rome Nota Interna No. 158, 1968 (unpublished).

[2] G. C. Fox, dissertation, Cambridge, 1967 (unpublished); T. W. Rogers, dissertation, Cambridge, 1967 (unpublished); G. C. Fox, E. Leader, and T. W. Rogers, in *Heildeberg International Conference on Elementary Particles*, edited by H. Filthuth (North-Holland Publishing Co., Amsterdam, 1968).

[3] G. Cohen-Tannoudji, A. Morel, and H. Navelet, Ann. Phys. (N. Y.) **46**, 239 (1968); S. Frautschi and L. Jones, Phys. Rev. **163**, 1820 (1967); **164**, 1918 (1967); J. D. Jackson and G. E. Hite, *ibid.* **169**, 1248 (1968).

[4] D. Z. Freedman and J. M. Wang, Phys. Rev. **160**, 1560 (1967).

[5] R. C. Arnold, Phys. Rev. Letters **14**, 657 (1965).

[6] A. Ahmadzadeh, Phys. Rev. Letters **20**, 1125 (1968).

[7] A. McKerrel and L. Sertorio, Nuovo Cimento **52A**, 1223 (1967); M. Barmawi, Phys. Rev. **166**, 1857 (1968).

More sophisticated study of the experimental[8] data together with the use of finite-energy sum rules (FESR)[9] has led to the elaboration of the concept of secondary trajectory and the determination of its kinematics in the particular case of the ρ'.[10] It is clear from the previously mentioned three general keystones of the Regge-pole hypothesis that we have to face a study of first trajectories and secondary trajectories and that the necessary method is the study of sets of reactions.

In Sec. 2 we summarize the customary kinematics. After an analysis of the experimental data (which has been summarized in Appendix B) we give in Sec. 3 the minimum configuration necessary to fit the present data. In Sec. 4 we discuss the results and list the experiments that we consider a crucial test for our present analysis.

2. FORMALISM

The formalism involves a catalog of the kinematics relevant to our reactions. We consider that the original work is sufficiently well-known that we need not summarize it in this paper. We will make use of t-channel helicity formalism with the following definitions:

$(1)+(2)\rightarrow(3)+(4)$ is the s-channel reaction;

$(1)+(\bar{3})\rightarrow(\bar{2})+(4)$ is the t-channel reaction.

In the t channel (1), $(\bar{3})$, $(\bar{2})$, and (4) will have helicities a, b, c, and d, respectively, and particle (1) will always be the pion ($a=0$).

Normalization:

$$\frac{d\sigma}{dt}=\frac{1}{16\pi}\frac{1}{S_{12}^2}\frac{1}{2j_1+1}\frac{1}{2j_2+1}\sum_{cdab} f_{cdab}f_{cdab}^*,$$

and for particle d the density matrix elements are defined by

$$\rho_{mm'}=\sum_{cab} f_{cmab}f_{cm'ab}^*/\sum_{cdab} f_{cdab}f_{cdab}^*,$$

while for particle b

$$\rho_{mm'}=\sum_{cda}(-1)^{m-m'}f_{cdam}f_{cdam'}^*/\sum_{cdab} f_{cdab}f_{cdab}^*,$$

$$S_{12}^2=[s-(m_1-m_2)^2][s-(m_1+m_2)^2],$$

$$s=2m_1E+m_1^2+m_2^2,\quad E=(p^2+m^2)^{1/2},$$

j_1, j_2 = spins of particles 1, 2.

(In our case $j_1=0$, $j_2=\frac{1}{2}$.)

First, write the helicity amplitude

$$f^t_{cdab}=(\cos\tfrac{1}{2}\theta_t)^{|\lambda+\mu|}(\sin\tfrac{1}{2}\theta_t)^{|\lambda-\mu|}\times K_{\lambda\mu}^{-1}(t)\beta_{cdab}(t)\sigma(t)(s_0{}^m)^{\alpha-M}A_{\lambda\mu}(\alpha), \quad (2)$$

where

$$\lambda=a-b,\quad \mu=c-d,\quad M=\max(|\lambda|,|\mu|),$$
$$\sigma=\text{either } i+\tan\tfrac{1}{2}\pi\alpha \quad \text{or} \quad -i+\cot\tfrac{1}{2}\pi\alpha.$$

These two cases belong to $\mp$ values of τ defined by

$$\sigma=(1+\tau e^{-i\pi\alpha})/\sin\pi\alpha,$$

where τ is the signature, a given trajectory $\alpha(t)$ has a definite value of τP, where P is the parity, β_{cdab} is the so-called reduced residue, $K_{\lambda\mu}(t)$ is the Wang factor,[11] $A(\alpha)$ is called the α matrix (see Appendix A). It is a rational function of $\alpha(t)$. Equation (2) is clearly an asymptotic formula which is valid up to terms of next order, for instance, a seconary pole.

Formula (2) does not uniquely define the contribution of one pole to $f_{cdab}{}^t$.

First, the factor $K_{\lambda\mu}{}^{-1}(t)$ has to be supplemented by further knowledge of the linear constraints at $t=0$. The satisfaction of the constraints at $t=0$ is either evasive or conspiring.[12]

Secondly, linear constraints at

$$t=(m_2\pm m_4)^2,\quad t=(m_1\pm m_3)^2 \quad (3)$$

must also be satisfied.

Thirdly, the $A(\alpha)$ factors may come from different mechanisms and for each value $0\leq\alpha$ for each pole we have several possible matrices $A_{\lambda\mu}(\alpha)$.

To study the above points, let us rewrite (2) in a slightly clearer way, namely,

$$f_{cdab}=\frac{SC}{(SC)_{\text{asymptotic}}}K_{\lambda\mu}{}^{-1}(t)(SC)_{\lambda\mu}\beta_{cdab}(t)\times\left(\frac{s}{s_0}\right)^{\alpha}A_{\lambda\mu}(\alpha)\sigma(t), \quad (4)$$

where

$$(SC)_{\lambda\mu}=s^{-M}(SC)_{\text{asymptotic}},$$
$$S=(\sin\tfrac{1}{2}\theta_t)^{|\lambda-\mu|},$$
$$C=(\cos\tfrac{1}{2}\theta_t)^{|\lambda+\mu|}.$$

Here "asymptotic" means the following: In the function of s, t, m_1, m_2, m_3, m_4, take the leading term in s. Now collect the kinematic factors and write

$$f_{cdab}=\frac{SC}{(SC)_{\text{asym}}}\gamma_{cd}{}'\gamma_{ab}{}'e^{-i(\pi/2)(\lambda-\mu)}\sigma(t)(s/s_0)^{\alpha},$$

where

$$\gamma_{cd}{}'=F_\mu(t)A_\mu[\alpha(t)]\gamma_{cd},$$
$$\gamma_{ab}{}'=F_\lambda(t)A_\lambda[\alpha(t)]\gamma_{ab}, \quad (5)$$

and we have factorized the factors in (4) as

$$K_{\lambda\mu}{}^{-1}(t)(SC)_{\lambda\mu}=F_\mu(t)F_\lambda(t)e^{-i(\pi/2)(\lambda-\mu)},$$
$$A_{\lambda\mu}(\alpha)=A_\lambda(\alpha)A_\mu(\alpha).$$

[8] J. Beaupre, R. Logan, and L. Sertorio, Phys. Rev. Letters **18**, 259 (1967).
[9] J. Beaupre and L. Sertorio, Nuovo Cimento **52A**, 1192 (1967).
[10] L. Sertorio and M. Toller, Phys. Rev. Letters **19**, 1146 (1967).
[11] L. L. Wang, Phys. Rev. **142**, 1187 (1966).
[12] By conspiracy we mean class III of Ref. 4. Classes I and II need not be distinguished and are called evasion here.

TABLE I. The factors $F(t)$. These are written for $t>0$ and in continuing to $t<0$, one should use the route $\sqrt{t}\to -i\sqrt{(-t)}$. The $F_{ab}(t)$'s are real for $t>(m_a+m_b)^2$, and imaginary quantities appear in the table because the upper thresholds have been ignored (see Appendix B).

		Evading	Conspiring
	(1) $\pi\pi$ vertex		
	F_{00}	1	$\sqrt{t}$
	(2) $\pi\omega$ vertex[a]		
$\tau P=+$	$F_0=0$		
	$F_1=-F_{-1}$	1	$\sqrt{t}$
$\tau P=-$	F_0	$(\sqrt{t})/T_{\pi\omega}$	$1/T_{\pi\omega}$
	$F_1=F_{-1}$	$1/T_{\pi\omega}$	$-(\sqrt{t})/T_{\pi\omega}$
	(3) $N\bar{N}$ vertex		
$\tau P=+$	$F_{\frac{1}{2}\frac{1}{2}}=F_{-\frac{1}{2}-\frac{1}{2}}$	i	$i\sqrt{t}$
	$F_{\frac{1}{2}-\frac{1}{2}}=F_{-\frac{1}{2}\frac{1}{2}}$	$i\sqrt{t}$	i
$\tau P=-$, (A_1)	$F_{-\frac{1}{2}\frac{1}{2}}=-F_{\frac{1}{2}-\frac{1}{2}}$	1	$\sqrt{t}$
$\tau P=-$, (π,B)	$F_{\frac{1}{2}\frac{1}{2}}=-F_{-\frac{1}{2}-\frac{1}{2}}$	$\sqrt{t}$	1
	(4) $N\bar{\Delta}$ vertex[b]		
	$F_{\frac{3}{2}\frac{1}{2}}$	ix	$i(\sqrt{t})x$
	$F_{\frac{1}{2}\frac{1}{2}}$	$i(\sqrt{t})x$	ix
	$F_{-\frac{1}{2}\frac{1}{2}}$	$i(\sqrt{t})x$	ix
	$F_{-\frac{3}{2}\frac{1}{2}}$	ilx	$i(\sqrt{t})x$

[a] The index on F is the helicity of the ω and $T_{\pi\omega}=\{[(m_\pi-m_\omega)^2-t][(m_\pi+m_\omega)^2-t]\}^{1/2}$.
[b] $x=[(m_\Delta-m_N)^2-t]^{-1}$ for $\tau P=+$; $x=[(m_\Delta-m_N)^2-t]^{-1/2}$ for $\tau P=-$.

In the evasive case F may be found from the work of Wang[11]; in Table I we repeat her results and also give the modifications due to the conspirational solution of the $t=0$ constraints. In this last case one must add the constraints relating the residues at $t=0$ of the two conspiring poles. The constraints on $\gamma'=F(t)A(t)\gamma$ are as follows.

Conspiracy Constraint

Unequal-mass vertices:

$$\gamma_{\lambda_{\bar{3}}\lambda_1}'|_{\tau P=+}=i\gamma_{\lambda_{\bar{3}}\lambda_1}'|_{\tau P=-}$$

for $\mathrm{sgn}\,[(m_1^2-m_3^2)(\lambda_1-\lambda_{\bar{3}})]>0$. There is no constraint for $\lambda_1-\lambda_{\bar{3}}=0$ and we have taken particle $\bar{3}$ as ω, $\bar{\Delta}$ for the $\pi\omega$, $N\bar{\Delta}$ vertices, respectively.

Equal-mass vertices:

No constraint on $\pi\pi$ vertex.

$N\bar{N}$ vertex:

$$\gamma'_{-\frac{1}{2}\frac{1}{2}}|_{\tau P=+}=\gamma'_{\frac{1}{2}\frac{1}{2}}|_{\tau P=-}.$$

Threshold Constraints

$\pi\omega$ vertex:

$$\sqrt{2}\gamma_1'=\gamma_0' \quad \text{at} \quad t=(m_\omega\pm m_\pi)^2;$$

$N\bar{\Delta}$ vertex:

$$\text{at } t=(m_N-m_\Delta)^2 \text{ only};$$

$\tau P=+$ (4 constraints):

$$\gamma'_{\frac{1}{2}\frac{1}{2}}=\gamma'_{-\frac{1}{2}\frac{1}{2}}=\sqrt{3}\gamma'_{\frac{3}{2}\frac{1}{2}}=\sqrt{3}\gamma'_{-\frac{3}{2}\frac{1}{2}},$$

$$\frac{d}{dt}[\sqrt{3}(\gamma'_{\frac{1}{2}\frac{1}{2}}-\gamma'_{-\frac{1}{2}\frac{1}{2}})-(\gamma'_{\frac{3}{2}\frac{1}{2}}-\gamma'_{-\frac{3}{2}\frac{1}{2}})]=0;$$

$\tau P=-$ (2 constraints):

$$\sqrt{3}(\gamma'_{\frac{1}{2}\frac{1}{2}}-\gamma'_{-\frac{1}{2}\frac{1}{2}})-(\gamma'_{\frac{3}{2}\frac{1}{2}}-\gamma'_{-\frac{3}{2}\frac{1}{2}})=0,$$

$$\gamma'_{\frac{1}{2}\frac{1}{2}}+\gamma'_{-\frac{1}{2}\frac{1}{2}}-\sqrt{3}(\gamma'_{\frac{3}{2}\frac{1}{2}}+\gamma'_{-\frac{3}{2}\frac{1}{2}})=0.$$

In interpreting the threshold constraints given above one must remember that moving a little way from $t=0$ and for $s\to\infty$, $SC/(SC)_{\text{asym}}\to 1$. The pseudothresholds (3) are for values of t far enough from $t=0$ that $SC/(SC)_{\text{asym}}$ does not appreciably differ from 1. To get formulas which exactly satisfy the threshold constraints in nonleading as well as leading order, it is necessary to include the nonasymptotic terms of the d^j matrix in our Regge expansion. Unfortunately, this then requires explicit consideration of daughters and compensating trajectories. We have calculated these effects and they are negligible near $t=0$. The effect from $t=0$ is very dependent on the slope and value of s_0 assumed for the daughter. We then consider the $s\to\infty$ limit in writing the pseudothreshold constraints. They are summarized above.

Finally, we have to consider the $A_{\lambda\mu}(\alpha)$ factors. More precisely, let us consider the $A(\alpha)$ matrices. For each pole we have a matrix belonging to $\alpha=1$ and a matrix belonging to $\alpha=0$. From Appendix A we see that in principle for each point we have five choices. Consequently, a theory with n poles allows in general $(5\times 5)^n$ different structures of the residues. Considering the additional kinematical option evasion-conspiracy, again in general we have $(2\times 5\times 5)^n$ different configurations of the joint structure of the residues due to the mentioned causes. It is consequently urgent to supplement the result of the formal reasoning with a concrete study of nature.

We would like to mention in this context that an attempt has been made[10,13] to connect $t=0$ symmetry and $A(\alpha)$ matrices. The idea is based on the conjecture that the amplitudes are functions of a parameter (e.g., the coupling constant) in such a way that a sense-nonsense value (e.g., $\alpha=0$) can be moved to $t=0$ with continuity. In such a way we use the $t=0$ symmetry predictions on the α factors. When we will discuss conspiracies we will favor this definite link.

The formalism introduced up to now is related to point (1) of the Introduction, namely, it is kinematic. We will not discuss here the formalism related to points (2) and (3) since we consider it to be generally known or easily found with appropriate references.

3. DISCUSSION AND RESULTS

It is clear that the kinematics leaves open a great variety of configurations. Also, the dynamical principles (2) and (3) are of very general nature and certainly not stringent enough for a derivation of the evaluation of

[13] M. Toller, in *Proceedings of the Fifth Coral Gables Conference on Symmetry Principles at High Energy*, edited by A. Perlmutter, C. A. Hurst, and B. Kursunoglu (W. A. Benjamin, Inc., New York, 1968).

the number of poles and determination of related residues and trajectories.

We will make additional free use of the principle of simplicity and economy in the framework outlined in the Introduction. We consider the principle of simplicity within the framework of the three general principles of Sec. 1, not as a practical guideline but as a true theoretical ingredient of the Regge-pole hypothesis. On the contrary, the principle of simplicity applied to a single reaction does not make sense.

Consider now the following scheme:

Reasonably well established features.

(1) Existence of the ρ pole;

(2) slope and intercept of the ρ trajectory,[9,14–16]

$$\alpha_\rho(t)=0.57+1.08t;$$

(3) existence of the ρ' pole.[8–10]

TABLE II. The quantity Q [defined in Eq. (6) of text]. This must be $\geqslant 0$ (if ω has spin 1) and is zero if but one $\tau P-$ particle is present (apart from nonasymptotic corrections and effects from averaging over a t interval). The evaluation of the error needs some statistical assumptions—the most important being that errors on density matrix elements are uncorrelated. In the following tables t_1 and t_2 are the range of t over which the data are averaged.

t_1	t_2	Q	Error
	(1) Q in $\pi N\to\omega\Delta$ at 3.5 GeV/c [a]		
−0.086	−0.2	0.1	0.03
−0.2	−0.4	0.076	0.029
−0.4	−0.6	0.06	0.027
−0.6	−0.8	0.08	0.045
	(2) Q in $\pi N\to\omega\Delta$ at 5 GeV/c [b]		
−0.053	−0.15	0.069	0.034
−0.15	−0.3	0.022	0.021
−0.3	−0.45	0.043	0.036
−0.45	−0.6	0.092	0.062
−0.6	−1.0	0.035	0.046
	(3) Q in $\pi N\to\omega\Delta$ at 8 GeV/c [c]		
−0.03	−0.15	0.033	0.025
−0.15	−0.3	0.003	0.017
−0.3	−0.6	0.04	0.028
−0.03	−0.1	0.053	0.04
−0.1	−0.2	0.018	0.015
−0.2	−0.3	0.006	0.039
−0.3	−0.45	−0.002	0.044
−0.45	−0.8	0.018	0.044
	(4) Q in $\pi N\to\omega N$ at 3.65 GeV/c [d]		
0.0	−0.2	0.039	0.032
−0.2	−0.5	0.012	0.032

[a] Reference 28.
[b] Reference 29.
[c] Reference 30.
[d] Reference 32.

TABLE III. The simplest theoretical configuration. ↓ indicates exchange degeneracy; → indicates conspiracy. The abbreviations C-S, C-NS, and C-fixed pole are explained at the end of Appendix B. First trajectories do not conspire, but are exchange-degenerate. Secondary trajectories do conspire, but are not exchange-degenerate.

First trajectories

0^-	π	$\alpha\to 0$	C-S[a]				
1^+	B	$\alpha\to 0$	C-S[b]	1^-	ρ	$\alpha\to 0$	C-NS[b]
2^-	↓			2^+	A_2	$\alpha\to 0$	C-NS[a]
3^+	↓			3^-	↓		

Secondary trajectories

0^-	π'	$\alpha\to 0$	C-NS[c]	$\to 0^+$	ϵ'	$\alpha\to 0$	C-NS[c]
1^+	B'	$\alpha\to 0$	C-fixed pole[d]	$\to 1^-$	ρ'	$\alpha\to 0$	C-fixed pole[d]
2^-				2^+	A_2'	$\alpha\to 0$	C-NS
3^+							

[a] Necessary.
[b] Follows from assumption of exchange degeneracy.
[c] Found empirically from the analysis of reactions (1′), (1″).
[d] Proposed by the $t=0$ symmetry continued to $t\neq 0$.

Less well established features.

(4) $\alpha_\rho\to 0$ is C-S.[17] Since the introduction of the ρ', the $\alpha_\rho\to 0$ C-S assignment is debatable. As a matter of fact, in Schmid's work[18] $\alpha_\rho\to 0$ C-NS is preferred.

(5) ρ' is conspiring. The assignment of conspiracy to the ρ' pole was based on the study of the πN charge-exchange (CEX) reaction. Two elements cooperate—a finite-energy sum rule[9,10] and the detailed t dependence of the experimental polarization data. Although the polarization experiment is of remarkable sophistication, it cannot quantitatively and unambiguously separate the different t behavior of a $\rho+\rho'$-conspiring model as opposed to the $\rho+\rho'$ model.

Suggested features.

(6) Although exchange degeneracy is not an exact symmetry, if there is any limit in which it becomes exact, the ρ and A_2 must then have the same ghost-eliminating mechanism at $\alpha=0$. It is then likely that even though their residues are no longer exactly proportional, the ρ and A_2 still retain the same $\alpha=0$ mechanism in the real world. Thus the $\rho-A_2$ exchange degeneracy suggests that both ρ and A_2 choose nonsense at $\alpha=0$.

The A_2 C-NS assignment is in agreement with high-energy data and finite-energy sum rules (FESR) in photoproduction,[19] KN,[20] and πN[21] elastic scattering. The FESR suggest that both A_2 and P' choose nonsense with an additional zero in the helicity-nonflip $N\bar{N}$ coupling. This extra zero presumably corresponds to the Höhler zero[15,22] in the $\rho\to N\bar{N}$ nonflip coupling in the context of exchange degeneracy. The high-energy

[14] M. Restignoli, L. Sertorio, and M. Toller, Phys. Rev. **150**, 1389 (1966).
[15] R. Dolen, D. Horn, and C. Schmid, Phys. Rev. **166**, 1768 (1968).
[16] C. B. Chiu, R. J. N. Phillips, W. Rarita, and R. J. Riddell, Phys. Rev. **165**, 1615 (1968).
[17] The abbreviations C-S and C-NS are explained at the end of Appendix A.
[18] C. Schmid, Phys. Rev. Letters **20**, 628 (1968).
[19] S.-Y. Chu and D. P. Roy, Phys. Rev. Letters **20**, 958 (1968).
[20] G. Dass and C. Michael, Phys. Rev. Letters **20**, 1066 (1968).
[21] V. Barger and R. J. N. Phillips, Phys. Rev. Letters **21**, 865 (1968).
[22] G. Höhler, J. Baacke, and G. Eisenbeiss, Phys. Letters **22**, 203 (1966).

data for $\pi^+p \to \eta^0\Delta^{++}$, $K^+p \to K^0\Delta^{++}$, and $K^-p \to \bar{K}^0 n$ has a characteristic slower falloff with t than the ρ exchange $\pi^-p \to \pi^0 n$, $\pi^+p \to \pi^0\Delta^{++}$. Then if the A_2 has a canonical slope of 1 we can rule out the Chew or no-compensating mechanisms (see Appendix A) which would give an extra zero in the $A_2 \to N\bar{\Delta}$ helicity-flip coupling. (Note that the density matrix elements of the Δ^{++} show that $K^+p \to K^0\Delta^{++}$ is dominated by helicity flip.)

(7) The exchange degeneracy $\pi - B$ involves a $\alpha_B \to 0$ C-S.

Consider now the status of the experimental data collection. It is important to establish a *hierarchy of experimental data.*

The accuracy of the data in the set (1) is in the following order:

TABLE IV. The couplings of the poles for the fit described in Appendix B. Notice the following technical differences from Eq. (5). (i) Units are $\hbar=c=\text{GeV}=1$. (ii) In order to get the couplings for the particular charge states observed one must multiply the tabulated γ's by a Clebsch-Gordon coefficient $C(T_1T_3T;\tau_1\tau_3)$ for particles of isospin T_1, T_3 coupling to a Regge pole of isospin T. τ_1, τ_3 are the t-channel components of isospin. (iii) The ρ' amplitudes have an extra factor $(s_0^{\rho'}/s_0^{B'})^{\alpha_{\rho'}(0)}$ to simplify the $t=0$ constraints. (iv) For all poles the $A(\alpha)$ had the $\alpha=0$, 1 structure specified in the text plus an extra factor $\frac{1}{2}(\alpha+1)(\alpha+2)$. The $\alpha+1$ is needed to eliminate a ghost and the $\frac{1}{2}(\alpha+2)$ is unimportant in the fit reported here.

Vertex	Coupling	Value
(1) The ρ Regge pole: $\alpha(t)=0.57+1.2t$; $s_0=0.98$		
$\pi\pi$	γ_{00}	9.13
$\pi\omega$	γ_1	$5.82+0.52t$
$N\bar{N}$	$\gamma_{\frac{1}{2}\frac{1}{2}}$	$-1.59-20t+16.2t^2$
	$\gamma_{-\frac{1}{2}\frac{1}{2}}$	-14
$N\bar{\Delta}$	$\gamma_{\frac{1}{2}\frac{1}{2}}$	$-0.24-3.17t$
	$\gamma_{\frac{3}{2}\frac{1}{2}}$	$0.62-18.3t$
	$\gamma_{-\frac{1}{2}\frac{1}{2}}$	$-2.5+8.66t$
	$\gamma_{-\frac{3}{2}\frac{1}{2}}$	10.4
(2) The ρ' Regge pole: $\alpha(t)=0.3+0.9t$; $s_0=0.46$		
$\pi\pi$	γ_{00}	-14.1
$\pi\omega$	γ_1	$3.97-20.9t$
$N\bar{N}$	$\gamma_{\frac{1}{2}\frac{1}{2}}$	7.73
	$\gamma_{-\frac{1}{2}\frac{1}{2}}$	-2.89
$N\bar{\Delta}$	$\gamma_{\frac{1}{2}\frac{1}{2}}$	$-1.45+6.12t$
	$\gamma_{\frac{3}{2}\frac{1}{2}}$	$-0.25+1.0t$
	$\gamma_{-\frac{1}{2}\frac{1}{2}}$	$-0.21-0.68t$
	$\gamma_{-\frac{3}{2}\frac{1}{2}}$	0.85
(3) The B Regge pole: $\alpha(t)=-0.5+t$; $s_0=0.069$		
$\pi\omega$	γ_0	$68.6-78.2t-127t^2$
	γ_1	194
$N\bar{N}$	$\gamma_{\frac{1}{2}\frac{1}{2}}$	36
$N\bar{\Delta}$	$\gamma_{\frac{1}{2}\frac{1}{2}}$	$3.17-32.6t$
	$\gamma_{\frac{3}{2}\frac{1}{2}}$	$-7.74-56.6t$
	$\gamma_{-\frac{1}{2}\frac{1}{2}}$	17.5
	$\gamma_{-\frac{3}{2}\frac{1}{2}}$	-51.4
(4) B' Regge pole: $\alpha(t)=0.3+t$; $s_0=3.13$		
$\pi\omega$	γ_0	$-12.9-3.94t$
	γ_1	$-2.82-9.12t$
$N\bar{N}$	$\gamma_{\frac{1}{2}\frac{1}{2}}$	-3.46
$N\bar{\Delta}$	$\gamma_{\frac{1}{2}\frac{1}{2}}$	1.18
	$\gamma_{\frac{3}{2}\frac{1}{2}}$	$1.0-3.84t$
	$\gamma_{-\frac{1}{2}\frac{1}{2}}$	$-0.85+4.58t$
	$\gamma_{-\frac{3}{2}\frac{1}{2}}$	-2.39

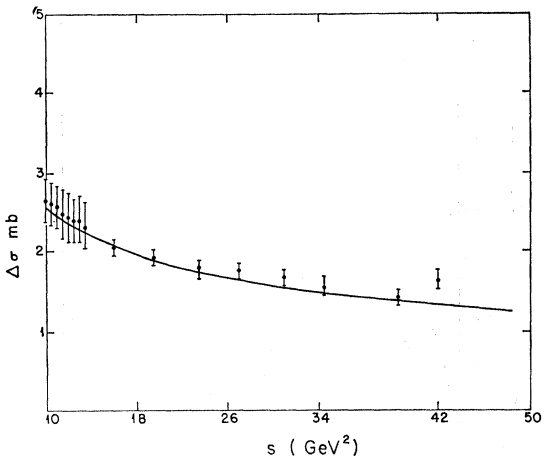

FIG. 1. The difference $\Delta\sigma=\sigma_- - \sigma_+$ of π^- and π^+ total cross sections plotted against s, the square of the c.m. energy.

(a) $\pi N \to \pi N$ CEX $d\sigma/dt$ [23,24] and $\sigma_- - \sigma_+$,[25,26]
(b) $\pi N \to \pi N$ CEX polarization,[27]
(c) $\pi N \to \omega\Delta$ existence of data at three energies,[28–30]
(d) $\pi N \to \pi\Delta$ existence of data at two energies,[30,31]
(e) $\pi N \to \omega N$ existence of data at two energies,[32,33]
(f) reactions known at only one energy. These are of less significance for the Regge-pole hypothesis.

By ordering the data, we obviously mean that each set of data has to be discussed and not simply used by the χ^2 criterion.

Thus if for a given reaction the various data have been consistently normalized, the χ^2 test of the theoretical formulas is meaningful. The bias introduced when the normalization uncertainty is much greater than the statistical errors may be accounted for either by increasing the errors of a suspect experiment or by allowing it an over-all scale factor (independent of t) to be varied and determined by the fit. Both of these methods have been used in our fit. For example, a

[23] M. A. Wahlig and I. Mannelli, Phys. Rev. **168**, 1515 (1968).
[24] P. Sonderegger *et al.*, Phys. Letters **20**, 75 (1966).
[25] A. Citron *et al.*, Phys. Rev. **144**, 1101 (1966).
[26] K. J. Foley *et al.*, Phys. Rev. Letters **19**, 330 (1967).
[27] P. Bonamy, P. Borgeaud, S. Brehin, C. Bruneton, P. Falk-Variant, O. Guisan, P. Sonderegger, C. Caverzasio, J. P. Guilland, J. Schneider, M. Yvert, I. Mannelli, F. Sergiampietri, and M. L. Vincelli, in *Heidelberg International Conference on Elementary Particles*, edited by H. Filthuth (North-Holland Publishing Co., Amsterdam, 1968).
[28] D. Brown, G. Gidal, R. W. Birge, R. Bacastow, S. Y. Fung, N. Jackson, and R. Pu, Phys. Rev. Letters **19**, 664 (1967).
[29] Bonn-Durham-Nijmegen-Paris-Strassbourg-Turin Collaboration, in Proceedings of the CERN Topical Conference on High-Energy Collisions of Hadrons, 1968 (unpublished).
[30] Aachen-Berlin-CERN Collaboration, Phys. Letters **19**, 608 (1965); **22**, 533 (1966); D. R. O. Morrison (private communication).
[31] Aachen-Berlin-Birmingham-Bonn-Hamburg-London (I.C.)-München Collaboration, Phys. Rev. **138**, B897 (1965); CERN Report No. 65-24 (unpublished).
[32] G. Benson, L. Lovell, G. T. Murphy, B. Roe, P. Sinclair, and J. Vander Velde (unpublished); G. Benson, thesis (unpublished).
[33] E. Shibata and M. Wahlig, Phys. Letters **22**, 354 (1966).

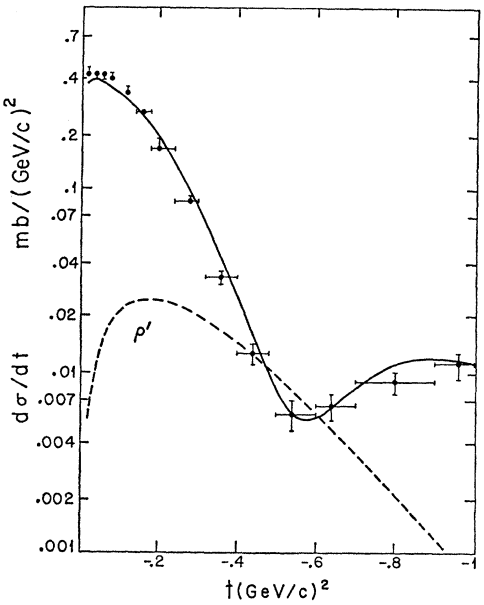

FIG. 2. $d\sigma/dt$ for πN CEX at lab momentum of 5.9 GeV/c.

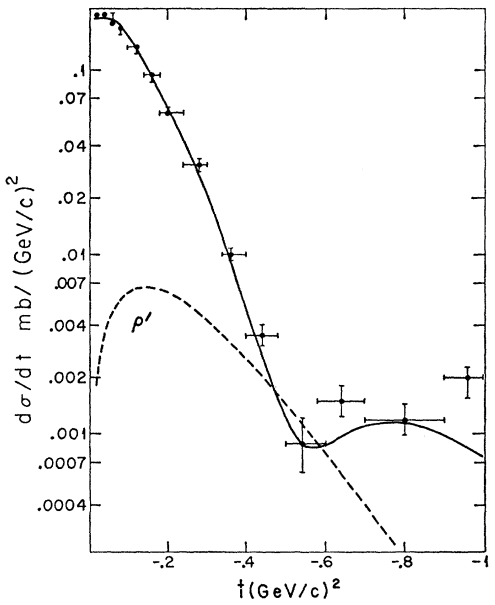

FIG. 4. $d\sigma/dt$ for πN CEX at lab momentum of 13.3 GeV/c.

problem arises in the $\pi N \to \omega\Delta$ reaction by considering the data at 4, 5, and 8 GeV/c which come from different experimental groups. This problem divides in two branches:

(a) Treating this reaction alone. If the data are biased in normalization, wrong values of the intercept of the various trajectories may be evaluated.

(b) Treating this reaction jointly, as we claim is necessary. In this case, for example, ρ and ρ' have stringent constraints from πN charge exchange. It is a delicate matter to understand if possible discrepancies among that evaluation and the $\pi N \to \omega\Delta$ data are due to a bias in $\pi N \to \omega\Delta$ or problems of the theory (see Appendix B).

Another uncertainty, of less importance but easier to correct, is that the sign of ρ_{31} and ρ_{10} depends on a conventional choice for the y axis defining the decay of the Δ and ω, respectively. Where this has not been specified in the experimental results, we have taken it in the direction $\mathbf{P}_\pi \times \mathbf{P}_\omega$ (or $\mathbf{P}_N \times \mathbf{P}_\Delta$) in the c.m. system.

From the above points we see that of our reactions only $\pi^- p \to \pi^0 n$ has negligible bias and even the next best known, $\pi N \to \omega\Delta$, has normalization uncertainties among the experiments at 4, 5, and 8 GeV/c lab momentum. Consequently, quantitative evaluations of intercepts from this experiment must be taken with a

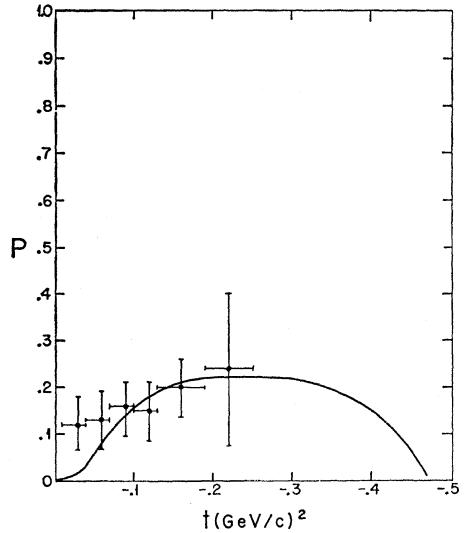

FIG. 3. πN CEX polarization at 5.9 GeV/c.

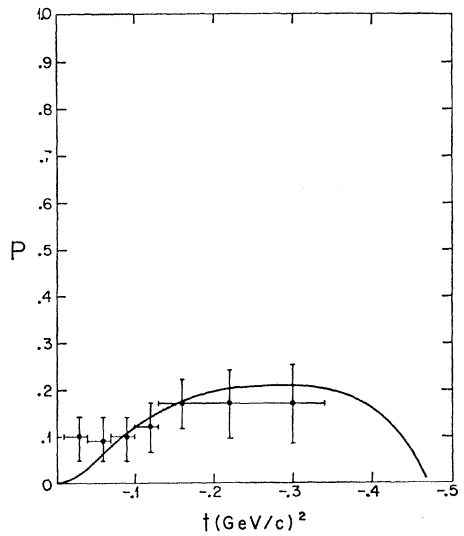

FIG. 5. πN CEX polarization at 11.2 GeV/c.

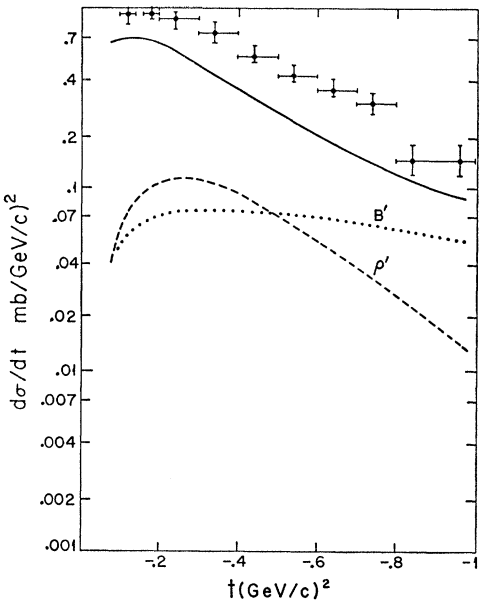

FIG. 6. $d\sigma/dt$ for $\pi N \to \omega\Delta$ at lab momentum of 3.5 GeV/c.

grain of salt while discrepancies between this reaction and the others will not be considered critical.

Let us consider in detail the $\pi N \to \omega\Delta$ reaction. Two quantities have a particular interest. The quantity

$$\rho_{00}{}^{\omega}\frac{d\sigma}{dt}=\frac{1}{16\pi}\frac{1}{S_{12}{}^{2}}\times\tfrac{1}{2}\sum f_{00ab}f^{*}{}_{00ab}$$

contains only the contribution of B-like poles, because 1^- particles do not couple to the $|00\rangle$ state of the

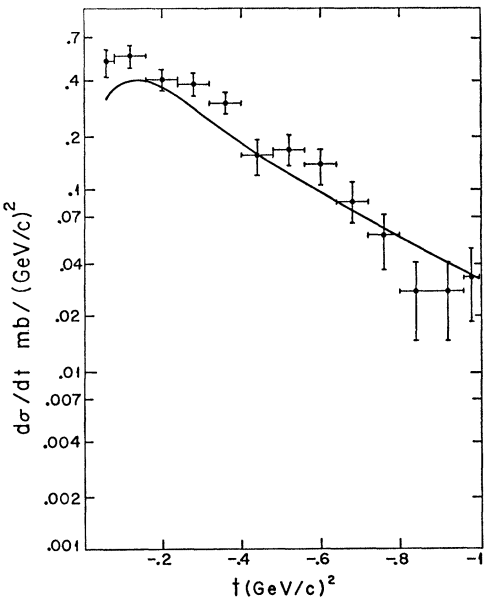

FIG. 7. $d\sigma/dt$ for $\pi N \to \omega\Delta$ at lab momentum of 5 GeV/c.

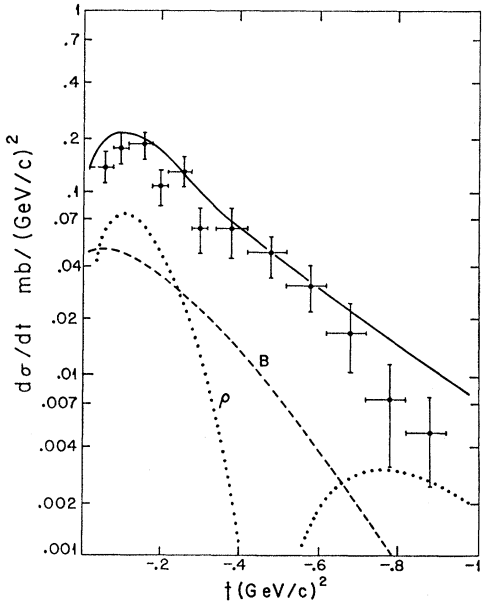

FIG. 8. $d\sigma/dt$ for $\pi N \to \omega\Delta$ at lab momentum of 8 GeV/c.

$|\pi\omega\rangle$ vertex. The quantity

$$Q=\rho_{00}(\rho_{11}-\rho_{1-1})-2\rho_{01}{}^{2} \qquad (6)$$

has the important property of being exactly zero in the limit $s\to\infty$ if only one 1^+ pole is contributing. At actual energies the identity is broken because of the factors $SC/(SC)_{\text{asym}}\neq 1$. But we know that by excluding a segment of the t axis surrounding the point $t=0$ the quantity $SC/(SC)_{\text{asym}}$ tends quickly to 1. With this caution the quantity Q is an indicator for the possible existence of secondary B poles also at intermediate energies.

The quantity Q is tabulated in Table II, and our use of these two quantities is described in Appendix B.

From the analysis reported in Appendix B, it is fairly easily recognized that the simplest theoretical configuration, as well as the most economical when all the three points mentioned in the Introduction are carefully considered, is that shown in Table III.

In proposing the above scheme we have combined

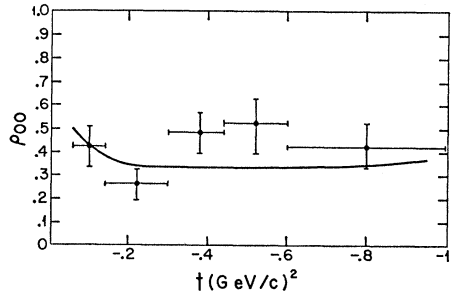

FIG. 9. The ω density matrix element $\mathrm{Re}\rho_{00}$ for $\pi N \to \omega\Delta$ at lab momentum of 5 GeV/c.

the work of this paper on reactions (1) with an analysis[34] of reactions (1′) and (1″) which involve π exchange. The latter analysis shows that neither π, A_1, or A_2 with an evading π, or $(\pi \to c)$, A_1, or A_2 with a conspiring π, is able to fit the data. The claim[35] that the latter model fits the data seems impossible without additional singularities in the j plane to satisfy the factorization constraints provided by the data on $NN \to N\Delta$ and $NN \to \Delta\Delta$. There are two distinct pole models that fit the data both of which have two important trajectories π and π' of pion-quantum

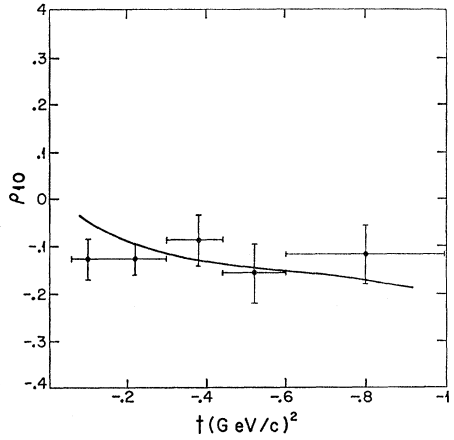

FIG. 10. The ω density matrix element $\mathrm{Re}\rho_{10}$ for $\pi N \to \omega\Delta$ at lab momentum of 5 GeV/c.

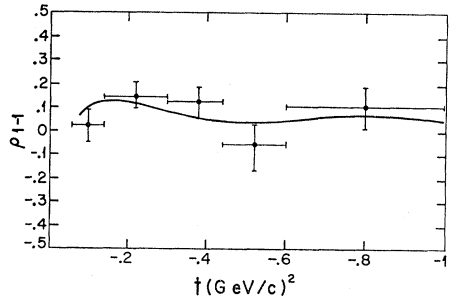

FIG. 11. The ω density matrix element $\mathrm{Re}\rho_{1-1}$ for $\pi N \to \omega\Delta$ at lab momentum of 5 GeV/c.

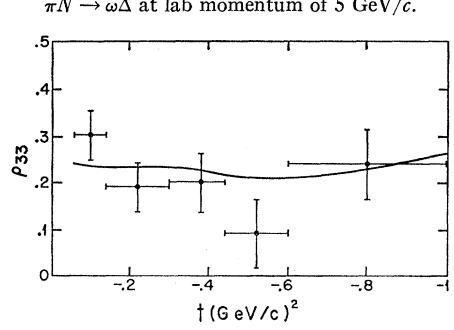

FIG. 12. The Δ density matrix element $\mathrm{Re}\rho_{33}$ for $\pi N \to \omega\Delta$ at lab momentum of 5 GeV/c.

[34] G. Fox (unpublished calculation). Also see the fit described in Table III of F. Arbab and J. W. Dash, Phys. Rev. **163**, 1603 (1967).

[35] F. Arbab and R. C. Brower, Phys. Rev. **175**, 1991 (1968).

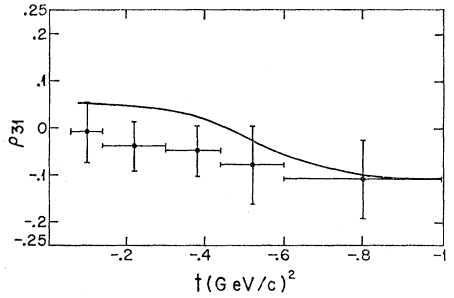

FIG. 13. The Δ density matrix element $\mathrm{Re}\rho_{31}$ for $\pi N \to \omega\Delta$ at lab momentum of 5 GeV/c.

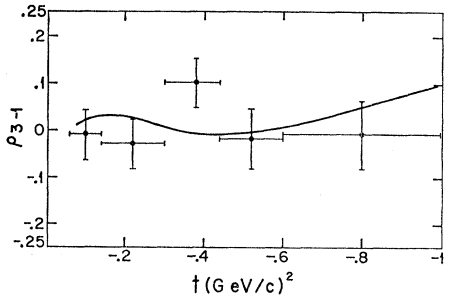

FIG. 14. The Δ density matrix element $\mathrm{Re}\rho_{3-1}$ for $\pi N \to \omega\Delta$ at lab momentum of 5 GeV/c.

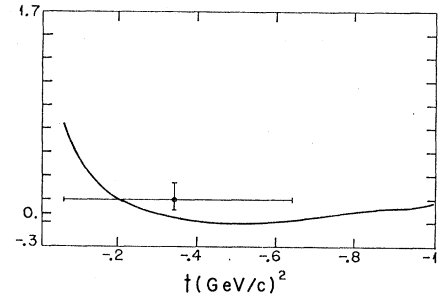

FIG. 15. The double correlation $\rho_{33}{}^{-}-\rho_{11}{}^{-}-2(\rho^{11}-\rho^{00})(\rho_{33}-\rho_{11})$ for $\pi N \to \omega\Delta$ at lab momentum of 5 GeV/c.

numbers and similar intercept. In one model π conspires and π' evades while in the other π' evades and the π conspires. These models are distinguished because the π has its pole of known magnitude while the π' is free. The first model, which we have chosen here, has the feature that the π' is about 20% of the π in the general case of unequal-mass reactions and only becomes the same size as the π in special cases, such as np charge exchange and photoproduction. The second model has the advantage of rescuing Mandelstam's derivation[36] of the Adler self-consistency relations from a pion conspiracy, which without the π' leads to disaster for unequal-mass vertices.[37] Both models give similar fits to the data and so it is sufficient to consider the first possibility here.

This configuration must indeed be supported by the

[36] S. Mandelstam, Phys. Rev. **168**, 1884 (1968).

[37] R. F. Sawyer, Phys. Rev. Letters **21**, 764 (1968).

numerical analysis. It is. The numerical analysis was made by several steps which are summarized in Appendix B. The trajectories are

$$\alpha_\rho(t)=0.57+1.2t, \quad \alpha_{\rho'}(t)=0.3+0.9t$$

and

$$\alpha_B(t)=-0.5+t, \quad \alpha_{B'}(t)=0.3+t.$$

The residues are tabulated in Table IV. The various observable quantities are plotted in Figs. 1–37, together with our fit denoted by a solid line. Dashed lines represent the contributions of separate poles.

Although other configurations are possible to find which also fit the data, they are less simple and economical. A short discussion of other possible configurations which we discard here is made in Appendix C.

The configuration which we have presented contains the following properties:

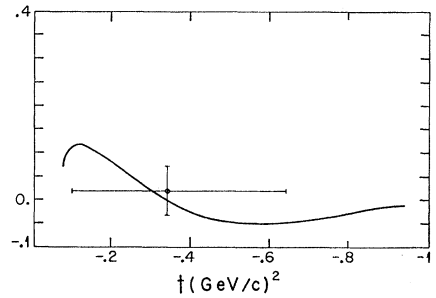

FIG. 16. The double correlation $\rho_{-}{}^{10}-2(\rho_{33}-\rho_{11})\rho^{10}$ for $\pi N \to \omega\Delta$ at lab momentum of 5 GeV/c.

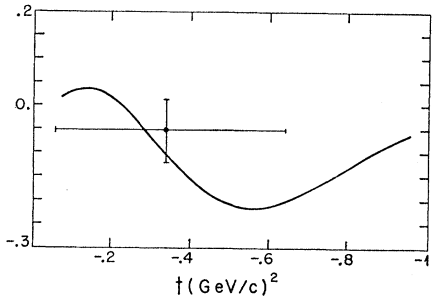

FIG. 17. The double correlation $\rho_{-}{}^{1-1}-2(\rho_{33}-\rho_{11})\rho^{1-1}$ for $\pi N \to \omega\Delta$ at lab momentum of 5 GeV/c.

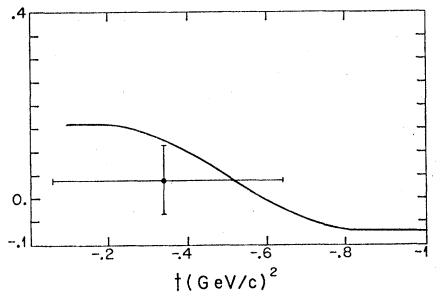

FIG. 18. The double correlation $\rho_{31}{}^{-}-2(\rho^{11}-\rho^{00})\rho_{31}$ for $\pi N \to \omega\Delta$ at lab momentum of 5 GeV/c.

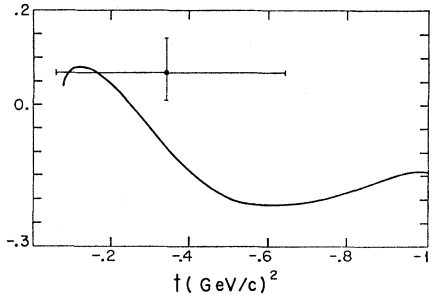

FIG. 19. The double correlation $\rho_{3-1}{}^{-}-2(\rho^{11}-\rho^{00})\rho_{3-1}$ for $\pi N \to \omega\Delta$ at lab momentum of 5 GeV/c.

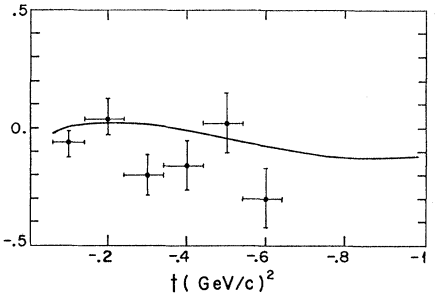

FIG. 20. The double correlation $\rho_{31}{}^{10}-\rho_{31}{}^{0-1}-2\rho^{10}\rho_{31}$ for $\pi N \to \omega\Delta$ at lab momentum of 5 GeV/c.

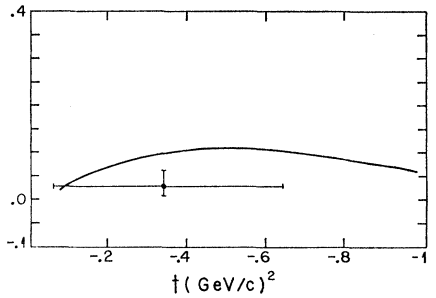

FIG. 21. The double correlation $\rho_{31}{}^{01}-\rho_{31}{}^{-10}-2\rho^{10}\rho_{31}$ for $\pi N \to \omega\Delta$ at lab momentum of 5 GeV/c.

(1) Kinematics.

Proposes the conspiracy (with the α factors implied by the group-theoretical approach) for secondary trajectories. Rejects the conspiracy among leading trajectories.

(2) Exchange degeneracy.

Confirms the validity of exchange degeneracy for leading trajectories. Rejects the exchange degeneracy for secondary trajectories. This breaking of exchange degeneracy is suggested not only by the experimental data, but also by Toller's work in Ref. 13.

(3) Sum rules.

The $\pi N-\pi N$ FESR are satisfied.[9,15] In particular, the $\alpha_\rho \to 0$ C-NS assignment is in accord with the

FESR of Ref. 18 for the $\pi\pi$ system and those of Gross[38] and Ademollo *et al.*[39] for $\pi\pi \to \pi\omega$.

4. COMMENTS

It seems to us that after the introduction of our configuration a new general discussion of the 1^+, 1^- exchange reactions is in order. We will make our comments again in line with the three keystone principles.

A. Kinematics

1. Behavior of the Residues

A feature valid only for the ρ pole is the constraint provided by the known residue at $t\sim 0.5$, where the

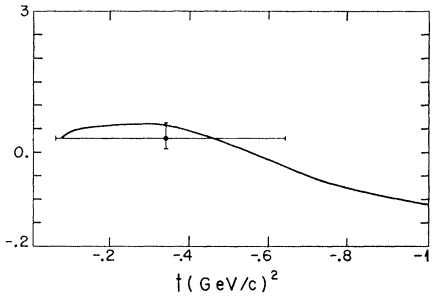

FIG. 22. The double correlation $\rho_{31}{}^{1-1}-\rho^{1-1}\rho_{31}$ for $\pi N \to \omega\Delta$ at lab momentum of 5 GeV/c.

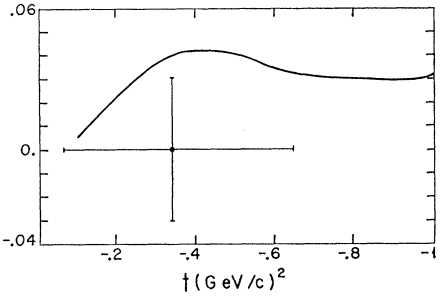

FIG. 23. The double correlation $\rho_{31}{}^{-11}-\rho^{1-1}\rho_{31}$ for $\pi N \to \omega\Delta$ at lab momentum of 5 GeV/c.

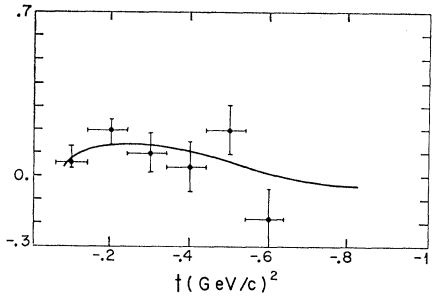

FIG. 24. The double correlation $\rho_{3-1}{}^{10}-\rho_{3-1}{}^{0-1}-2\rho^{10}\rho_{3-1}$ for $\pi N \to \omega\Delta$ at lab momentum of 5 GeV/c.

[38] D. J. Gross, Phys. Rev. Letters **19**, 1302 (1967).
[39] M. Ademollo, H. R. Rubinstein, G. Veneziano, and M. A. Virasoro, Phys. Rev. Letters **19**, 1402 (1967).

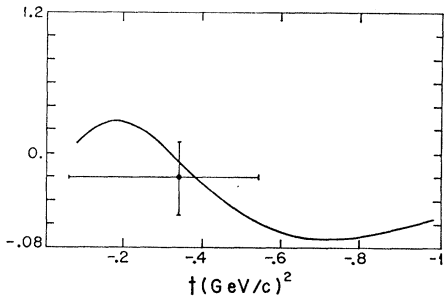

FIG. 25. The double correlation $\rho_{3-1}{}^{01}-\rho_{3-1}{}^{-10}-2\rho^{10}\rho_{3-1}$ for $\pi N \to \omega\Delta$ at lab momentum of 5 GeV/c.

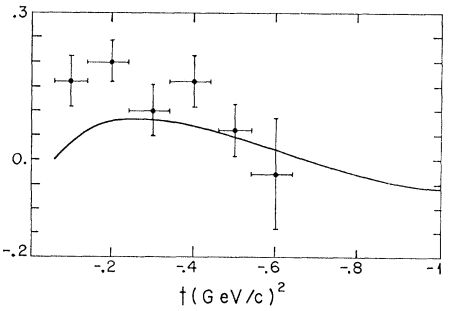

FIG. 26. The double correlation $\rho_{3-1}{}^{1-1}-\rho^{1-1}\rho_{3-1}$ for $\pi N \to \omega\Delta$ at lab momentum of 5 GeV/c.

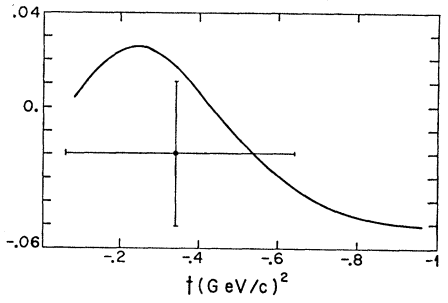

FIG. 27. The double correlation $\rho_{3-1}{}^{-11}-\rho^{1-1}\rho_{3-1}$ for $\pi N \to \omega\Delta$ at lab momentum of 5 GeV/c.

trajectory creates the actual ρ particle. In this way we can estimate the $\rho \to \pi\pi$, $\rho \to \pi\omega$,[40] and $\rho \to N\bar{N}$ couplings at this point. Indeed, if one uses factorization and a constant ratio for $\gamma_{\pi\pi}{}^3/\gamma_{\pi\omega}{}^3$, one finds too large a ρ contribution to $\pi N \to \omega N$ and $\pi N \to \omega\Delta$ in terms of both the energy dependence of the data and the dip in $d\sigma/dt$ near $t\sim -0.6$ (see Appendix B). This effect is more pronounced if the ρ chooses sense at $\alpha=0$, which is one of our reasons for preferring the ρ nonsense at $\alpha=0$ solution.

Another very interesting feature is that the residue $\gamma_{\pi\omega}{}^{\rho'}(t)$ has a t dependence very different from the $\gamma_{\pi\pi}{}^{\rho'}(t)$ residue. This is necessary in order to explain why there is appreciable dip in $\pi^- p \to \pi^0 n$, $\pi^+ p \to \pi^0\Delta^{++}$ (i.e., ρ larger than ρ' here) but little dip in $\pi^+ p \to \omega^0\Delta^{++}$,

[40] M. Gell-Mann, D. Sharp, and W. G. Wagner, Phys. Rev. Letters **8**, 261 (1962).

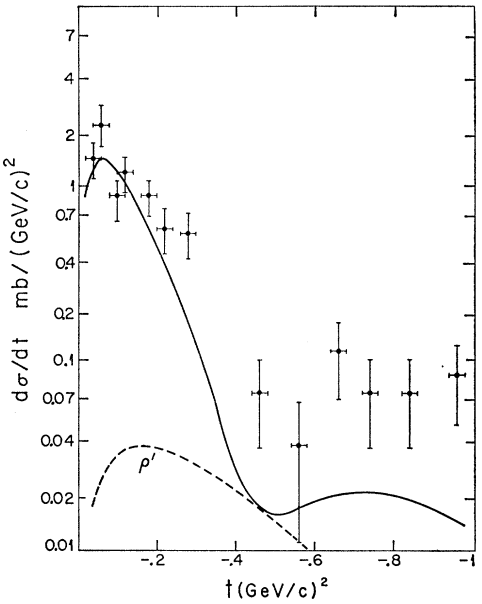

FIG. 28. $d\sigma/dt$ for $\pi N \to \pi\Delta$ at lab momentum of 4 GeV/c.

$\pi^+ n \to \omega^0 p$. This is ensured in our model by making $\gamma_{\pi\omega^\rho}/\gamma_{\pi\pi^\rho}$ decrease and $\gamma_{\pi\omega^{\rho'}}/\gamma_{\pi\pi^{\rho'}}$ increase with increasing $-t$. But we would like to remark that the fact that the $\pi\omega$ amplitude is stronger than the $\pi\pi$ amplitude at increasing energies is perhaps consistent with very reasonable models for Regge trajectories at high energies t.

2. *Conspiracies*

There is an important distinction in the role of the pairs (π',c'), (ρ',B'). From an analysis of reactions

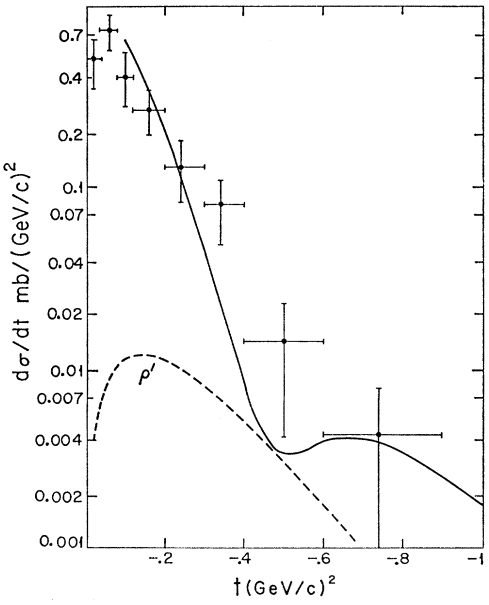

FIG. 29. $d\sigma/dt$ for $\pi N \to \pi\Delta$ at lab momentum of 8 GeV/c.

(1′) and (1″) one finds that the signs and magnitudes of the (π',c') residues are strongly correlated to the π as they attempt to reproduce the absorptive-model fits to these reactions which we can view as an evading π (as in our model) plus a π-Pomeranchuk cut dynamically generated from it. However, in this spirit the (ρ',B') pair is more naturally associated with the ρ-Pomeranchuk cut than that due to B-Pomeranchuk. This may make one disbelieve the model since with the present experimental data there is no compelling argument for (or against) it (see Appendix D).

B. Exchange Degeneracy

Although the doublet $(\rho'-B')$ is not exchange-degenerate with $(\pi'-c')$ (i.e., there is not a unique degenerate Lorentz pole), the structure of the secondary trajectories is still the most simple simply because they are doublets. Unfortunately, however, this circumstance

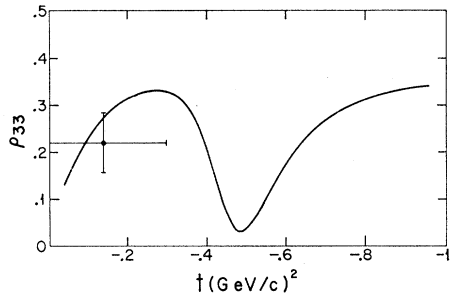

FIG. 30. The Δ density matrix element $\mathrm{Re}\rho_{33}$ for $\pi N \to \pi\Delta$ at lab momentum of 8 GeV/c.

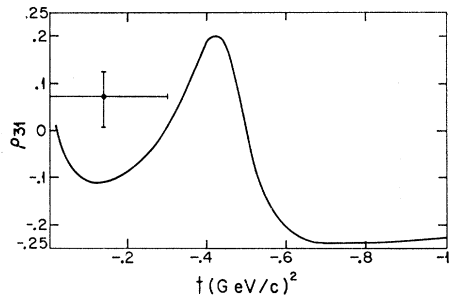

FIG. 31. The Δ density matrix element $\mathrm{Re}\rho_{31}$ for $\pi N \to \pi\Delta$ lab momentum of 8 GeV/c.

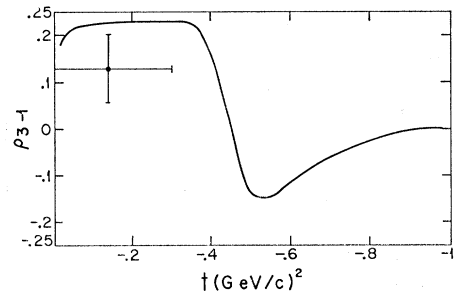

FIG. 32. The Δ density matrix element $\mathrm{Re}\rho_{3-1}$ for $\pi N \to \pi\Delta$ lab momentum of 8 GeV/c.

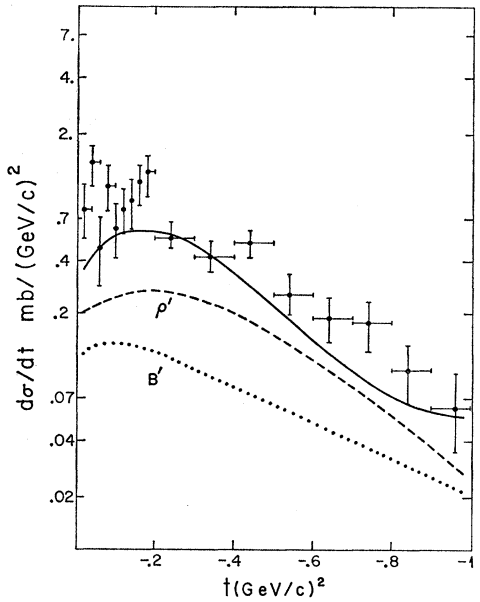

FIG. 33. $d\sigma/dt$ for $\pi N \to \omega N$ at lab momentum of 3.6 GeV/c.

breaks the exchange degeneracy. We think it important to stress this point.

C. Sum Rules

A consequence of sum rules has been recently proposed by Chew and Pignotti.[41] Reactions with resonating final (states, particles) (ω, Δ in our study) have complementary description in terms of multi-Regge exchange. As a matter of fact, our remark in

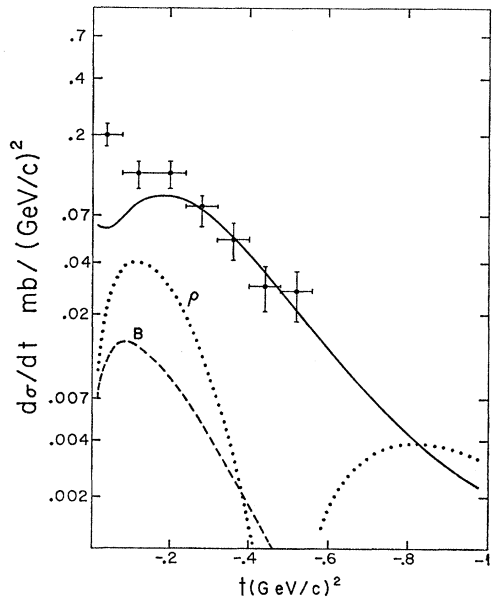

FIG. 34. $d\sigma/dt$ for $\pi N \to \omega N$ at lab momentum of 10 GeV/c.

[41] G. F. Chew and A. Pignotti, Phys. Rev. Letters **20**, 1078 (1968).

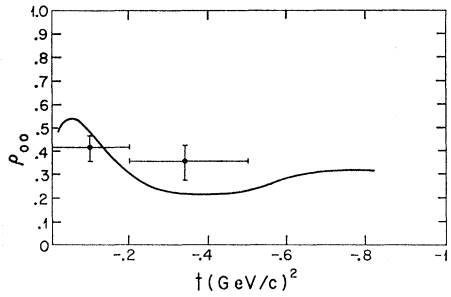

FIG. 35. The ω density matrix element $\mathrm{Re}\rho_{00}$ for $\pi N \to \omega N$ at lab momentum of 3.6 GeV/c.

Sec. 1 that two-body reactions are not necessarily more fundamental than others has a close bearing on this point. We did not analyze the interplay between our treatment of secondary trajectories of the two-body formalism with the many-body approach, but we desire to stress the importance of this fact here.

Predictions and Suggestions

We predict the existence of a B'. Our fit favors $\alpha_{B'} \to 1$ C-NS. Consequently, the predicted particle should be a 3^+. A straight-line behavior of the B' trajectory is in accord with a mass of

$$m_{B'}{}^2 \cong 2.7 \text{ GeV}^2.$$

Notice that our model predicts the existence of a A_2' particle sitting on the c' trajectory. By assuming that a linear behavior of the trajectory is followed, the mass of the A_2' can be predicted to be roughly

$$m_{A_2'}{}^2 = 2.1 \text{ GeV}^2.$$

Moreover, the Regge structure of the A_2' residues is determined to be conspiracy and C-NS. From this we can make rather interesting predictions. The $\pi^- p \to \eta n$ reaction has to have a measurable polarization. The t behavior of the polarization must be similar to the πp CEX polarization, i.e., it must have an extra zero in t

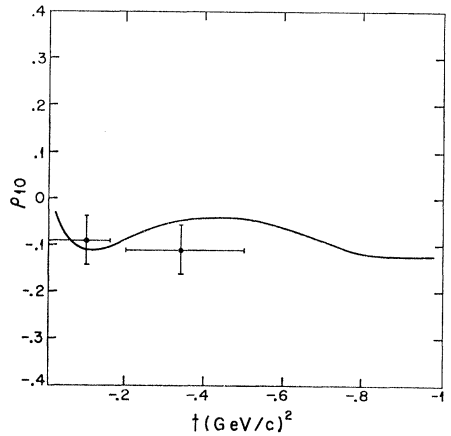

FIG. 36. The ω density matrix element $\mathrm{Re}\rho_{10}$ for $\pi N \to \omega N$ at lab momentum of 3.6 GeV/c.

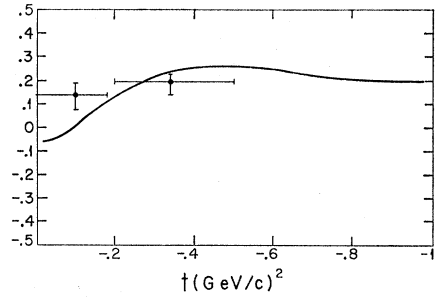

FIG. 37. The ω density matrix element $\mathrm{Re}\rho_{1-1}$ for $\pi N \to \omega N$ at lab momentum of 3.6 GeV/c.

near the forward direction. Yet the α factors for A_2' and ρ' are different. The energy dependence of the neutron polarization is predicted to be

$$P(s)\sim\frac{s^{\alpha_{A2}+\alpha_{A'2}}}{s^{2\alpha_{A2}}+s^{2\alpha_{A'2}}+s^{\alpha_{A2}+\alpha_{A'2}}}\sim s^{\alpha_{A'2}-\alpha_{A2}}\sim s^{-0.5}.$$

Needless to say, an accurate measurement of the neutron polarization in the $\pi^- p \to \eta n$ reaction, although relatively simple in comparison to resonance production experiments, will be of a primary importance for checking our proposed configuration of Regge secondary trajectories.

Polarization measurements in $\pi^- p \to \pi^0 n$ and $\pi^- p \to \eta n$ are of particular interest as they provide direct tests of the vanishing at $t=0$ of the ρ' contribution to $\pi^- p \to \pi^0 n$, which is a consequence of a conspiracy involving just two poles (ρ', B'), whereas a cut would presumably have no such extra zero.

Apart from the general plea for more accurate experiments (using, if possible, the same method of separating resonance and background contributions at each energy in order to render the normalizations directly comparable), some other particularly useful tests would be

(i) More data on $\pi N \to \omega N$ and $\pi N \to \pi\Delta$ to tighten the restrictions of factorization.

(ii) Measurements of ρ_{00} near the forward direction in $\pi N \to \omega N$ and $\pi N \to \omega\Delta$. $\rho_{00} \to 0$ if we have only conspiring poles (B', ρ') but $\to 1$ if we have only evading poles (ρ, B). In the analogous reactions of set (1'), $\pi N \to \rho N$ and $\pi N \to \rho\Delta$, $\rho_{00} \to$ const (neither 1 nor 0) as $t \to 0$, allowing a direct estimation of the relative contributions of conspiring and evading poles.

(iii) Measurements of the double correlations for the joint decay of ω and Δ at further energies (we only know of such data at 5 GeV/c[29]) will provide checks on the t factors and factorization. Figures 15–27 give our fit to the 5-GeV/c data. The most directly useful quantities are ρ_{33}^-, ρ_{31}^-, and ρ_{3-1}^- from which one can determine the $\tau P = -$ couplings to the $N\bar{\Delta}$ vertex. Quantities such as ρ_{3-1}^{1-1}, ρ_{3-1}^{-11} are sensitive to the nonasymptotic corrections to the Regge formulas.

ACKNOWLEDGMENTS

Thanks are due to D. R. O. Morrison and J. C. Vander Velde for providing important unpublished experimental data. We are grateful to Dr. C. Kaysen for his hospitality at the Institute for Advanced Study. It is also a pleasure to acknowledge the friendly assistance of Princeton Computer Center.

APPENDIX A: α FACTORS CONTAINED IN THE RESIDUES IN ORDER TO PRESERVE THEIR ANALYTICITY

The study of the α structure of the residues covers part of the ghost-eliminating program, namely, that part which does not involve compensating trajectories.

In the case of boson trajectories the singularities included in the residues are for α=integer. These factors are properties of the coupling of the trajectory to the various vertices. Because of factorization we can write the α factors in matrix form (2×2) in which rows and columns belong respectively to the vertex λ and vertex μ. We indicate as "sense vertex" the situation

$$\alpha \geqq |\lambda| \quad \text{or} \quad |\mu|$$

and as nonsense vertex the situation

$$\alpha < |\lambda| \quad \text{or} \quad |\mu|.$$

Let us consider the point $\alpha=0$.

For odd-signature trajectories (as we have in this study) of both natural $(\tau P=+)$ and unnatural parity $(\tau P=-)$, $\alpha=0$ is a wrong-signature point. We have then a full variety of matrices. They are usually identified in the following way:

1. Choosing sense $\begin{vmatrix} 1 & \sqrt{\alpha} \\ \sqrt{\alpha} & \sqrt{\alpha}\sqrt{\alpha} \end{vmatrix}$

2. Choosing nonsense $\begin{vmatrix} \sqrt{\alpha}\sqrt{\alpha} & \sqrt{\alpha} \\ \sqrt{\alpha} & 1 \end{vmatrix}$

3. Chew $\alpha\times\begin{vmatrix} 1 & \sqrt{\alpha} \\ \sqrt{\alpha} & \sqrt{\alpha}\sqrt{\alpha} \end{vmatrix}$

4. No-compensating trajectory $a\times\begin{vmatrix} \sqrt{\alpha}\sqrt{\alpha} & \sqrt{\alpha} \\ \sqrt{\alpha} & 1 \end{vmatrix}$

5. Choosing sense with a wrong-signature fixed pole $\begin{vmatrix} 1 & 1/\sqrt{\alpha} \\ 1/\sqrt{\alpha} & 1/\sqrt{\alpha}\sqrt{\alpha} \end{vmatrix}$

The $A_{\lambda\mu}(\alpha)$ factors are the products of the previous matrices by the α factors belonging to the asymptotic $E_{\lambda\mu}{}^{\alpha+}(\theta_t)$ functions and they represent the final structure of the residues.

The corresponding catalog of the A matrices is

1. Choosing sense $\begin{vmatrix} 1 & \alpha \\ \alpha & \alpha\alpha \end{vmatrix}$

2. Choosing nonsense $\begin{vmatrix} \alpha & \alpha \\ \alpha & \alpha \end{vmatrix}$

3. Chew

$$\alpha\times\begin{vmatrix}1 & \alpha\\ \alpha & \alpha\alpha\end{vmatrix}$$

4. No-compensating trajectory

$$\alpha\times\begin{vmatrix}\alpha & \alpha\\ \alpha & \alpha\end{vmatrix}$$

5. Choosing sense with a wrong-signature fixed pole

$$\begin{vmatrix}1 & 1\\ 1 & 1\end{vmatrix}$$

In the text we refer to cases 1, 2, and 5 as C-S, C-NS, and C-fixed pole, respectively.

APPENDIX B: DISCUSSION OF THE PROPOSED CONFIGURATION

The major property of the configuration under discussion is that it is the simplest possible for the set of reactions (1). This remark automatically *answers* the major criticism of the Regge-pole hypothesis, namely, that there is no precise rule for a restriction on the number of poles.

Before explaining why this configuration best explains our experimental knowledge, let us remember a few simple concepts.

At the present state of development, trajectories and residues are quantities having a role somewhat similar to that of parameters. We try to find the maximum restrictions on them. When we speak of residues we refer to the factorized entity $\gamma_{ab}'=F_{ab}(t)A_{ab}(t)\gamma_{ab}(t)$. The observable quantities are constructed with products of γ'. The total cross sections are bilinear and all other quantities are quadrilinear expressions. But any of these expressions are correct only if the constraints listed in Sec. 3 are taken into account.

While the energy dependence is mainly explained by the knowledge of the trajectories (s^α factors), the momentum-transfer dependence is a combination of (a) dependence due to $s_0^{-\alpha(t)}$, (b) $A(t)$ factors, (c) $F(t)$ factors, relevant for taking into account the $t=0$ and threshold behavior and $t=0$ constraints, and (d) threshold constraints, effective on the t dependence of $\gamma(t)$. All of these points are of equal importance. Our task is to prove that we can separately evaluate them. The technique is to study the importance of the four factors in the several steps of the fitting procedure together with the following scheme of reasonings.

1. πN CEX Reaction

Data from 5–22 GeV/c were used.[23–27]

a. Sum Rules

The FESR for $t=0$ are the most accurate. This sum rule favors the ρ' *conspiracy*. Two remarks are relevant. First, with the actual precision of the experimental data, by using the evaluation of Ref. 16 for the integral from threshold to $\bar{\nu}$, there is agreement between ρ' conspiring and both the sum rule and the data on $\sigma_-(\nu)-\sigma_+(\nu)$ (see Fig. 1). Second, when extremely precise total cross-section data become available, care should be taken in expressing the sum-rule consistency

$$\frac{\text{Born}+\int_{\text{thr}}^{\bar{\nu}}[\sigma_-(\nu)-\sigma_+(\nu)]p_{\text{lab}}(\nu)d\nu}{p_{\text{lab}}(\bar{\nu})[\sigma_-(\bar{\nu})-\sigma_+(\bar{\nu})]}=\frac{\bar{\nu}}{\alpha^\rho+1}$$

and

$$2m_N p_{\text{lab}}(\bar{\nu})[\sigma_-(\bar{\nu})-\sigma_+(\bar{\nu})]=-\gamma_{00}{}'^\rho\gamma_{\frac{1}{2}\frac{1}{2}}{}'^\rho(\nu/s_0)^{\alpha(0)},$$

where

$$\nu=\tfrac{1}{2}(s-u).$$

In the spirit of Dolen, Horn, and Schmid we know that the Regge amplitude "interpolates" the data in any energy region in which resonances occur. This region could be any energy. The expression of the sum-rule consistency is consequently nontrivial. Study is in progress on this subject.

b. Differential Cross-Section Dip

The $\alpha_\rho\to 0$ C-NS assignment changes the older description of the dip due at the point $\alpha_\rho=0$. In particular the contribution of the ρ' is required to be stronger than in Ref. 10 for increasing values of $-t$. In this way one gets an evaluation of $s_0{}^{\rho'}$.

c. Crossover

The Höhler zero[15,22] in the non-spin-flip ρ residue is effected by the existence of the ρ', which is in this amplitude of similar size to the ρ at present energies. However, the relative size of $\gamma_{\frac{1}{2}\frac{1}{2}}{}'^\rho$ at $t=0$ (known from total cross section) and at $t=m_\rho{}^2$ (known from form-factor data) is well known to need a strong variation in t of $\gamma_{\frac{1}{2}\frac{1}{2}}{}'^\rho$. This suggests a zero in $\gamma_{\frac{1}{2}\frac{1}{2}}{}'^\rho$ near $t=0$ but this may be for $t>0$ or $t<0$, the ρ' having the possibility of moving the effective zero $t\approx-0.1$. In view of the many possibilities available, we have fixed a zero in $\gamma_{\frac{1}{2}\frac{1}{2}}{}'^\rho$ at $t=-0.075$ and have tolerated a fit which slightly violates the expected value of $\gamma_{\frac{1}{2}\frac{1}{2}}{}'^\rho$ at $t=m_\rho{}^2$. Notice that the sign of the polarization and the known relative sign of the ρ couplings at $t=m_\rho{}^2$ ($\gamma_{\frac{1}{2}\frac{1}{2}}{}'/\gamma_{\frac{1}{2}-\frac{1}{2}}{}'>0$) predicts destructive interference between ρ and ρ' for $t<0$ if $\gamma_{\frac{1}{2}\frac{1}{2}}{}'^\rho$ has not changed sign by then. This is interesting because similar destructive interference occurs between π and π' in NN CEX and photoproduction. At larger $-t$ values, c' and ρ interference may help to explain the difference between the pairs

$$np\to pn,\quad p\bar{p}\to n\bar{n}$$

and

$$pp\to\Delta^{++}\Delta^0,\quad p\bar{p}\to\Delta^{++}\bar{\Delta}^{++}.$$

Meanwhile it has been suggested in Ref. 6 that the interference between ω and its secondary trajectory will explain the crossover in $K^\pm p$ and pp, $p\bar{p}$ elastic scattering.

d. Sign of the Polarization

The polarization is always >0. The energy behavior is very flat, which favors $\alpha_{\rho'}(0)>0$. It follows that $A(\alpha)$ matrices of type 2, 3, and 4 (Appendix A) are excluded. This is considered as evidence for $\alpha_{\rho'}\to 0$ C-fixed pole (as in Ref. 10). This result involves, via conspiracy, the $\alpha_{B'}\to 0$ C-fixed pole.

2. $\pi N\to\omega\Delta$ Reaction

Data at 3.5, 5, and 8 GeV/c were used.[28–30] For the ρ and ρ' poles there is a flow of information from the πN CEX reaction. The assignments specifying the B and B' trajectories come by exclusion (our consideration of other possibilities may be found in Appendix C) and by considering the following reasoning.

a. Quantity Q

First of all we consider

$$Q=\rho_{00}(\rho_{11}-\rho_{1-1})-2\rho_{10}^2.$$

This is a sensor for B' as described in the text. Table III provides some indication for the *existence of* B'. Then either of the two B-like poles is the candidate for conspiring with ρ'; let us call the conspiring pole B'. Consequently $F^{B'}(t)$ and $A^{B'}(t)$ are fixed.

b. Tests for B

A first discussion on the B and B' poles can be made by analyzing the quantities

$$\rho_{00}\frac{d\sigma}{dt},\quad(\rho_{11}-\rho_{1-1})\frac{d\sigma}{dt},\quad\rho_{10}\frac{d\sigma}{dt}.$$

The first one only contains the helicity-zero couplings of 1^+ poles. The others only get contributions from $\tau P=-$ poles, but this is only exact in the asymptotic $s\to\infty$ limit. In particular, the second quantity picks out just the helicity-one part of $\tau P=-$ contributions. Having tied down the B' parameters rather stringently through the conspiracy conditions, the above-mentioned quantities are sensitive to the B alone. The t dependence of the data better favors B evasive and is consistent with $\alpha_B\to 0$ C-S. This last assignment is mostly suggested by exchange degeneracy and consequent over-all simplicity. If the data provided by different experimental groups at pion energies of 4, 5, and 8 GeV/c are consistent, a rather precise evaluation of $\alpha_B(0)$ is possible. The present data require $\alpha_B(0)$ to be in the range from -0.3 to -0.5.

c. $\tau P=+$ Poles

To examine the ρ and ρ' one may take

$$(\rho_{11}+\rho_{1-1})d\sigma/dt,$$

which again asymptotically only contains $\tau P=+$ contributions. By taking a single averaging $\tau P=+$ pole one finds $\alpha_{\tau P=+}(0)\sim 0$. This result, which is slightly inconsistent with the πN CEX analysis, shows a similarity with the $\tau P=-$ separate analysis, namely, $\alpha_{\tau P=-}\sim -0.5$ is lower than expected. More than considering these facts as a difficulty we interpret them as a very possible discrepancy among the experimental normalizations. In fact, when presenting the χ^2 table in Sec. 4 of this Appendix, it is understood that the data at 3.6 GeV/c of π momentum have an over-all normalizing factor which turns out to be 0.69. The detailed structure of the $N\bar{\Delta}$ residue functions is less easily studied than the $\pi\omega$ residue functions. In fact such quantities as $\rho_{33}d\sigma/dt$, involving the Δ matrix elements, get contributions from both values of τP. Further measurements of the double correlations[42] such as ρ_{33}^{00} will improve the situation. Figures 15–27 contain our fit to the 5-GeV/c double-correlation data.

d. Constraints for $t\neq 0$

While for the πN reaction the constraint at $t=4m_N^2$ is not relevant for our analysis, in the unequal-mass reactions the $t\neq 0$ constraints are very important. Since the factors $F(t)$ and $A(t)$ are assigned for all the four poles ρ, ρ', B, and B' with reasonable accuracy in the preceding discussion (which involves also knowledge of the four trajectories), the $t\neq 0$ constraints carry the last t dependence which is left in the structure of the $\gamma'(t)=F(t)A(t)\gamma(t)$. In order that the constraints become linear functions of the varied parameters the $\gamma(t)$ are expressed as polynomials in t with an over-all exponential dependence given by the scale factor s_0. The constraints contain as coefficients the $F(t=t_0)$ and $A(t=t_0)$ (t_0 being the threshold point), which makes them rather complicated functions of α. But this causes only minor technical difficulty in finding the derivatives of the amplitudes which are needed by the fitting program.

Finally, we should specify that we have included both threshold constraints for the $\pi\omega$ vertex [i.e., at $t=(m_\pi+m_\omega)^2$ and $t=(m_\pi-m_\omega)^2$, which means $t\approx 0.85$ and $t\approx 0.4$, respectively], but only the pseudothreshold $t=(m_N-m_\Delta)^2\approx 0.09$ constraints for the $N\bar{\Delta}$ vertex. These constraints plus the conspiracy constraints lead to a total of some 20 constraints among the approximately 48 parameters expressing the polynomials $\gamma(t)$.

Further constraints are provided by such things as the known ρ couplings at $t=m_\rho^2$.

e. Consequences of the Constraints (at $t=0$ and the Thresholds)

The conspiracy condition is such that for an elastic reaction the relative signs of the unfactorized couplings at $t=0$ implies a negative coupling constant when t reaches the value of the (mass)^2 of the particle to be created, unless one residue function changes its sign. We have achieved this sort of crossover by making the

[42] H. Pilkuhn and B. E. Y. Svensson, Nuovo Cimento 38, 518 (1965).

B' $\alpha \to 1$ C-NS. In the old conspiring π configuration, one similarly made the π conspirator (usually called c) choose nonsense at $\alpha_c = 0$.

A more interesting point is that the threshold constraints, in Table II, relate helicity amplitudes which appear as bilinear products in the density matrix elements. Then once one has prescribed the t dependence through the $A(t)$ and $F(t)$ factors, one can calculate the signs of ρ_{10}, ρ_{31}, and ρ_{3-1}. If this is violated by experiment, the indication is then found for an extra zero between threshold and $t=0$ in the residue functions not given by $A(t)$ or $F(t)$. For instance, in $\pi N \to \rho N$ and $\pi N \to \rho\Delta$ one has $\rho_{10}<0$, which is just right for a conspiring π, and similarly the signs of $\pi N \to \rho\Delta$, $NN \to N\Delta$, and $NN \to \Delta\Delta$ are correctly predicted. [However, see Appendix D for a comment on why a (π evasive, $c' \to \pi'$) configuration is still necessary.] In our reaction $\pi N \to \omega\Delta$ we have experimentally $\rho_{10}<0$ which can be predicted by an evasive B $\alpha \to 0$ fixed pole whereas a conspiring B $\alpha \to 0$ fixed pole predicts the wrong sign. In the configuration discussed here the B contribution does not make a clear-cut prediction. In fact, near $t_0=(m_\pi - m_\omega)^2$ it happens that $\alpha_B \approx 0$ makes the $\gamma_{10}'(t_0) \approx 0$. This implies γ_{00}' also very small because the constraint is $\sqrt{2}\gamma_{10}' = \gamma_{00}'$, which is satisfied by a $0=0$ solution.

3. $\pi N \to \pi\Delta$ Reaction

Data at 4 GeV/c [31] and 8 GeV/c [30] were used. It is a pity that there are not more data on this reaction since, although ρ and ρ' both contribute, ρ is the dominant pole[43] and more data would allow a rather accurate determination of the $\rho \to N\bar{\Delta}$ residue functions.

The density matrix elements of the Δ are known to agree roughly with the Stodolsky-Sakurai prediction

$$\rho_{33}=\tfrac{3}{8}, \quad \rho_{3-1}=\tfrac{1}{8}\sqrt{3}, \quad \rho_{31}=0.$$

As has been shown,[2,44] this may be deduced from the kinematic constraints at $t=(m_N-m_\Delta)^2 \approx 0.09$ (see Table II). In fact, putting $\gamma_{\frac{1}{2}\frac{1}{2}}' \approx 0$ (as is necessary in order to have the dip of $d\sigma/dt$ at $t=0$) and neglecting the small helicity-flip-2 coupling $\gamma_{-\frac{3}{2}\frac{1}{2}}'$, the remaining helicity-flip-1 residues are related at $t \approx 0.09$ by

$$\gamma_{\frac{3}{2}\frac{1}{2}}' = -\sqrt{3}\gamma_{-\frac{1}{2}\frac{1}{2}}'.$$

Assuming that this equation remains true in the physical $t<0$ region, one derives the Stodolsky-Sakurai distribution. This can hardly be viewed as a success for the theory since it expresses the fact that the kinematical singularities of the t-channel amplitudes have overwhelmed the dynamical information. In such cases where there are no important dynamical t-channel effects near $t=0$ (such as the pion pole), it would be useful to express the density matrix elements with reference to different set of axes in defining the decay angles θ and φ. Such sets are occasionally used in the literature,[45] like the "helicity frame" (where one has a formula for the density matrix elements involving s-channel helicity amplitudes instead of t-channel ones) or the "Adair frame." Both these cases do not have t-channel threshold singularities.

[43] M. Krammer and U. Maor, Nuovo Cimento **50A**, 963 (1967).
[44] L. Jones, Phys. Rev. **163**, 1530 (1967).

TABLE V. χ^2 data for 4-pole 4-reaction fit.

Reaction	Data points	χ^2
πN CEX	127	297
$\pi N \to \omega\Delta$	171	331
$\pi N \to \pi\Delta$	36	72
$\pi N \to \omega N$	30	83
Total	364	783

4. $\pi N \to \omega N$ Reaction

Data at 3.6 [32] and 10 GeV/c [33] were used. As there was much uncertainty in the normalization of these experiments (especially at 10 GeV/c), the experimental data at both energies were allowed a normalization factor, determined by the fit. Consequently, the figures presented show a poor agreement between data and theory. By multiplying the data at 3.6 and 10 GeV/c by factors 0.75 and 0.76, respectively, one obtains agreement with the theoretical curves. The χ^2 table which follows is written under such convention. The data at 10 GeV/c do not show a dip near zero, and this discrepancy with all the other experiments cannot be explained by the theory; nevertheless we do not consider this a serious problem.

From factorization one makes statements about the density matrix elements for $\pi N \to \omega N$ similar to those already made for $\pi N \to \omega\Delta$. However the data are still too rough to allow any detailed deductions.

5. Comments on Table V

In Table V we present the χ^2 of our fit for the various reactions. Of course, better fits to each individual reaction may be obtained than those given by the joint fit. Also almost half the χ^2 in $\pi N \to \omega N$ comes from the lowest t point at 10 GeV/c—a discrepancy mentioned in the text. The rather large χ^2 for πN CEX was due to slight differences between the data of Refs. 23 and 24.

APPENDIX C: OTHER POSSIBLE CONFIGURATIONS

The main reason for this appendix is that the approximation of the experimental knowledge allows a certain freedom in our conclusions discussed previously. Although it is theoretically required to study sets of reactions, the experimental data for any given set should be known with the same degree of consistency

[45] A random experimental reference is the discussion following the review talk of E. Lohrmann at the 1967 Stanford conference, Deutsches Elektronen-Synchrotron Report No. DESY 67/40 (unpublished).

common in a single experiment. Because it is not so, a few comments are in order.

As a first instance, the study of reactions 2, 3, and 4 in (1) provides good evidence for the existence of a ρ' but is consistent with either a conspiring or evading ρ'. The necessity for the conspiring choice is indicated by the πN CEX reaction. Also for this reaction the present data, although in support of the ρ' conspiracy assignment, are not in full contradiction with an evasive ρ'.

We have analyzed the "$B+B'$ both evasive" configuration by taking a single B (averaging the two B's) and studying the $A(\alpha)$ matrix corresponding to it. The fit to the $\pi N \to \omega\Delta$ reaction alone found the best choice for the $\alpha \to 0$ A matrix to correspond to the C-fixed pole assignment. The configuration was, for all poles nonconspiring,

$$\begin{aligned} &\rho \quad \alpha \to 0 \quad \text{C-NS}, && \alpha_\rho(t)=0.58+t,\\ &\rho' \quad \alpha \to 0 \quad \text{C-fixed pole}, && \alpha_{\rho'}(t)=-0.04+1.09t,\\ &B \quad \alpha \to 0 \quad \text{C-fixed pole}, && \alpha_B(t)=-0.49+0.73t. \end{aligned}$$

$\chi^2=225$ on 125 data points belonging to the reaction $\pi N \to \omega\Delta$ at 4, 5, and 8 GeV/c momentum (double correlations excluded).

We do not consider this configuration particularly relevant. We have considered the $A(\alpha)$ C-fixed pole as supporting the hypothesis of two B trajectories of which one is conspiring. Within the above framework we have compared various $A(\alpha)$ matrices for the ρ (cases 1, 2, and 5 of Appendix A). In the case 1, $\alpha_\rho \to 0$ C-S, the fit to $\pi N \to \omega N$ and $\pi N \to \omega\Delta$ found the t dependence due to the ρ contribution objectionable, in that it adjusted the scale factor s_0 to be small [$\sim$0.1 GeV^2] that it gave negligible contribution to both reactions at present energies.

Obviously another configuration is possible for all poles nonconspiring:

$$\begin{aligned} &\rho \quad \alpha \to 0 \quad \text{C-NS}, && B \quad \alpha \to 0 \quad \text{C-S},\\ &\rho' \quad \alpha \to 0 \quad \text{C-fixed pole}, && B' \quad \alpha \to 0 \quad \text{C-fixed pole}. \end{aligned}$$

This configuration differs from that developed earlier in the text only as regards the secondary trajectories which are here nonconspiring. This configuration will give also a very good fit. The reason for this statement is that this configuration contains more freedom because both trajectories and residues of ρ' and B' are uncorrelated at $t=0$. In addition, the $\alpha_{\rho'} \to 0$ C-fixed pole assignment, not being justified by the group-theoretical reasoning following from the conspiring choice, makes this configuration very uneconomical from the theoretical point of view.

An interesting possible configuration, proposed in Ref. 6, which we would like to mention is

$$\begin{array}{llllll} & \rho \text{ nonconspiring} & & & & \\ c & \alpha \to 0 & \text{C-NS} \to \pi & \alpha \to 0 & \text{C-S}, \\ \downarrow & & \downarrow & & \\ \rho' & \alpha \to 0 & \text{C-NS} \to B & \alpha \to 0 & \text{C-S}, \end{array}$$

where the parity doublets (c,π), (ρ',B) are exchange degenerates. In this way a single exchange-degenerate Lorentz pole would contain two leading trajectories with general simplicity.

Such an hypothesis meets the following difficulties:

(1) Since c should be $\alpha \to 0$ C-NS, the same assignment, if involved for ρ', is due to exchange degeneracy. But the group-theoretical reasoning predicts $\alpha \to 0$ C-fixed pole for ρ'. Consequently, a superimposed zero, beyond the $t=0$ symmetry prediction, must be invoked for the ρ'-pole residues in order to restore the exchange degeneracy.

(2) Additionally, a ρ' with $\alpha \to 0$ C-NS either predicts an unobserved zero in the πN CEX polarization or implies $\alpha_{\rho'}(0)<0$ or a very small slope of the ρ' trajectory.

(3) Analysis of the reactions (1′) and (1″) shows an inconsistency with the $\pi \to c$ model (even after adding the A_1). The reasons have been outlined in paragraph 3 of the main text.

(4) The analysis of $\pi N \to \omega\Delta$ shows that ρ' $\alpha \to 0$ C-NS $\to B$ $\alpha \to 0$ C-S is clearly rejected. An important reason is that a single B having the same intercept as the ρ' does not give a good fit to $\rho_{00}d\sigma/dt$. This is illustrated by the first fit discussed in this appendix, namely when the $\rho'-B$ conspiracy condition is released the ρ' and B intercepts move apart.

As a last configuration consider

$$\begin{aligned} &\rho \quad \alpha \to 0, \quad \text{C-S}\\ &\rho' \quad \alpha \to 0, \quad \text{C-fixed pole} \to B \quad \alpha \to 0 \quad \text{C-fixed pole} \end{aligned}$$

and no exchange degeneracy condition.[10] Even though this was preferable to the simpler Amadzadeh hypothesis just discussed, the fit was still poor. (The best χ^2 obtained is 275 for the same data points as in the first fit discussed.) Moreover, in such a fit, very rapid variation of the residues was required so that there was little remnant of conspiracy.

APPENDIX D: REGGE CUTS

Prejudices against secondary Regge poles can always find encouragement in the possible existence of Regge cuts. However, as mentioned in the text, it is notoriously difficult to detect their characteristic energy dependence and one may consider the violation of factorization exhibited by reactions (1), (1′), (1″) as evidence for cuts. From this point of view the ρ' with its high intercept just represents the ρ-Pomeranchuk cut and one may soon expect the ρ'' of lower intercept to appear as a representative of the B-Pomeranchuk cut.

Reactions going via pion exchange are also affected by secondary Regge trajectories. The best configuration $\{\pi, (\pi' \to c')\}$ contains the additional doublet trajectories π' and c' just in order to satisfy the factorization requirements for the sets of reactions (1′) and (1″). Yet this complicated configuration is able to fit the

data no better than the absorptive model. As a matter of fact, if the amplitudes had just a pion pole and residue obeying the threshold plus $t=0$ conditions but not factorization, these would be good amplitudes as far as fitting data is concerned. A single Regge pole with factorization has anomalies which either a π cut or a $(\pi' \to c')$ doublet is called upon to fix.

As an illustration of this remark, remember our comment in Appendix B that the $(\pi \to c)$ model predict the right sign and shape of $\rho_{10}{}^{\rho}(t)$, of which the dominant part is proportional to $\gamma_0{}^{\pi\to\pi\rho}\gamma_1{}^{\pi\to\pi\rho}$.

In the $\{\pi,(\pi' \to c')\}$ model ρ_{10} is dominated by the term containing the product $\gamma_0{}^{\pi\to\pi\rho}\gamma_1{}^{\pi'\to\pi\rho}$ and there appears no obvious sign prediction (as the threshold constraints now operate separately for π and π'). However, the correct sign is generated if the π and π' destructively interfere in the $\lambda_\rho=0$ amplitudes. Such destructive interference between π and π' runs through all the reactions (1′) and (1″).

Let us discuss for a moment the existence of Regge cuts from a very general point of view. If a clear-cut mechanism for generating cuts by the known and established Regge poles (ρ,B,π in our discussion) existed, interesting schemes could be imagined. Although it is not the only mechanism which can be devised, consider the Mandelstam mechanism in which the Pomeranchuk interacts with a given Regge pole generating a corresponding cut. A general scheme then follows which is summarized in Fig. 38. The left and right schemes are possibly exchange degenerate. A Regge pole has been surrounded by a circle to distinguish it from a cut. Such a mechanism creates a cut which can be divided artificially in two pieces labelled by $\tau P=+$ and $\tau P=-$. This is the meaning of the horizontal lines. Then two extra contributions from each pole (ρ,B,A_2,π) are expected.

It is obvious that we could have introduced such a

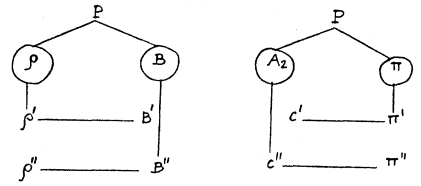

FIG. 38. Diagram illustrating relationship between cuts and poles discussed in Appendix D.

configuration in our fit, obtaining curves not significantly different from those belonging to the configuration proposed in the text and shown in the figures. In other words, we do not believe that the s-channel experimental data at the present moment can distinguish between the two configurations. One might then argue that the secondary Regge trajectories introduced were just simply simulating these cuts. The answer is twofold.

First, remember that a true Regge-pole contribution must satisfy factorization while a pole simulating a cut does not. In particular, the conspiracy concept disappears and a pole simulating a cut would not have any zeros at $t=0$ except those coming from analyticity. An argument in favor of the ρ' being a true Regge pole is found in the πN CEX reaction. In fact, an originally successful ρ cut,[46] able to fit the πN CEX polarization, was subsequently found to be in poor agreement with the FESR[9] unless one added the extra $t=0$ zero coming naturally from a conspiracy involving poles.

Secondly, if the ρ', B', and A_2' particles are found as predicted by the present study, a very strong argument against cuts exists. If, instead, the particles are clearly rejected by experiment, it is very possible that the mentioned cut configuration is true.

[46] C. B. Chiu and J. Finkelstein, Nuovo Cimento 48, 820 (1967).